

***Paranita*, a new genus of spiders from northeastern Argentina (Araneae, Trachelidae)**

Martín J. RAMÍREZ* & Cristian J. GRISMADO

División Aracnología, Museo Argentino de Ciencias Naturales “Bernardino Rivadavia”– CONICET, Av. Ángel Gallardo 470, C1405DJR, Buenos Aires, Argentina. *Corresponding autor: ramirez@macn.gov.ar

Abstract: *Paranita*, a new spider genus in the family Trachelidae, is described with two new species, *Paranita paulae* sp. n. and *Paranita inesae* sp. n., both from grasslands and marshes of the Paraná and Uruguay Rivers in northeastern Argentina. *Paranita* species are similar to those of the genera *Orthobula* and *Capobula* in having abundant spines on the tibia, metatarsus and tarsus of the two pairs of anterior legs, as well as large pores on the surface of the carapace and a peculiar morphology of the claw lever of the legs. However, phylogenetic analysis of molecular sequences and morphological data suggests that *Paranita* is not closely related to those genera and, therefore, these similarities would be evolutionary convergences.

Key words: Dionycha, phylogenetics, taxonomy, South America

Resumen: *Paranita*, un nuevo género de arañas del noreste argentino (Araneae, Trachelidae). Se describe *Paranita*, un nuevo género de arañas de la familia Trachelidae, con dos nuevas especies, *Paranita paulae* sp. n. y *Paranita inesae* sp. n., ambas de pastizales y bañados de los Ríos Paraná y Uruguay en el noreste de Argentina. Las especies de *Paranita* son similares a las de los géneros *Orthobula* y *Capobula* por tener abundantes espinas en las tibias, metatarsos y tarsos de los dos pares de patas anteriores, además de grandes poros en la superficie del carapacho y una morfología peculiar del esclerito elevador de las uñas de las patas. Sin embargo, el análisis filogenético de los datos de secuencias moleculares y de la morfología sugieren que *Paranita* no está cercanamente emparentado a aquellos géneros y, por lo tanto, esas similitudes serían convergencias evolutivas.

Palabras clave: Dionycha, filogenia, taxonomía, Sudamérica

INTRODUCTION

Flood plains are highly dynamic and diverse ecosystems that are usually under a high anthropic pressure (Tockner *et al.*, 2008). The wetlands of the Paraná River Delta are, in particular, currently faced with serious conservation challenges, with an estimated of one third of the freshwater marshes lost in a short period between 1999 and 2013 (Sica *et al.*, 2016). These habitats harbor a rich spider fauna, including endemic species adapted to grasses and the long-leaved plants of marshes (Ceccarelli *et al.*, 2019). Among these species there are beautiful minute spiders of the family Trachelidae, commonly found in the temporarily flooded areas of the Paraná River, from Buenos Aires to Chaco and Misiones, and in some localities of the adjacent Uruguay River basin. They are small, shiny reddish spiders with a design of chevrons on the

dorsal opisthosoma, common in the riparian vegetation near ponds or flooded areas. We describe here both species in the new genus *Paranita*.

The spiders now grouped in the family Trachelidae have a fluctuating taxonomic history, shifting their affiliation to the families Clubionidae, Corinnidae, Liocranidae, or Phrurolithidae (see Bosselaers & Jocqué, 2002; Haddad & Lyle, 2008; Ramírez, 2014; Wheeler *et al.*, 2017; Haddad *et al.*, 2021). A conspicuous characteristic of many trachelid spiders is the virtual absence of spines on the legs; instead, many species, and more often the adult males, have short, blunt macrosetae, called cusps. Several trachelids, however, have leg spines in addition to the cusps (for example, *Meriola* Banks, 1895, see Platnick & Ewing, 1995, González-Márquez *et al.*, 2021; *Spinotrachelas* Haddad, 2006; *Afroceto* Lyle and Haddad, 2010; *Poachelas* Haddad and Lyle, 2008), and yet oth-

ers have numerous spines and no traces of cusps (*Orthobula* Simon, 1897 and *Capobula* Haddad, Jin, Platnick and Booysen, 2021, see Wheeler *et al.*, 2017, Haddad *et al.*, 2021). The new species *Paranita paulae* also has leg spines and no cusps, and it was included in our previous phylogenetic analyses based on morphology (Ramírez, 2014) or genomic plus morphological data (Azevedo *et al.*, 2022a), under the name “Trachelidae ARG” and “cf. *Orthobula* sp.”, respectively. These phylogenetic analyses suggested that they belong to the family Trachelidae despite their atypical morphology. Beyond the conspicuous leg spines, these undescribed trachelids are also similar to *Orthobula* and *Capobula* by the deep pits covering the carapace. In absence of the leg cusps, which could be a synapomorphy, or at least a diagnostic character of some trachelids, the microscopic morphology of the adhesive setae on the tip of the legs (the claw tuft) and their interaction with the tarsal claws is also informative for their kinship (Ramírez, 2014; Azevedo *et al.*, 2022a, b). The trachelids have a characteristic morphology of the sclerite that bears the claws (the claw lever), interlocking with the base of the claw tuft setae, a mechanism that probably allows the muscular operation of the claw tufts (Ramírez, 2014).

In this contribution we propose the new trachelid genus *Paranita*, describe two new species from the northeast of Argentina, and study their relationships, in particular with *Orthobula* and *Capobula*, using genetic and morphological data.

MATERIAL AND METHODS

Specimens are deposited in the National Collection of Arachnology, Museo Argentino de Ciencias Naturales “Bernardino Rivadavia”, Buenos Aires, Argentina (MACN-Ar), Cátedra de Artrópodos, Facultad de Ciencias Exactas y Naturales de la Universidad Nacional del Nordeste, Corrientes, Argentina (CARTROUNNE), and Museo de La Plata, Argentina (MLP). Coordinates were taken in the field with GPS and transcribed literally as in labels or added a posteriori using Google Earth; in the last case, they are reported between brackets. Habitat data from labels are provided without translation. The map of geographic records was made with SimpleMappr (Shorthouse, 2010). Most specimens were collected in the riparian vegetation near ponds or flooded areas (Fig. 1). Specimens of *P. paulae* were collected in high numbers by careful examination of grass bases

and their accumulated leaf litter (Fig. 1E).

For scanning electron microscope images (SEM) the samples were gradually dehydrated to 100% ethanol, critical point dried and coated with gold-palladium, and examined in a FEI-XL30 under high vacuum, with accelerating voltages 10–20 kV, using a secondary electron (SE) detector. Female genitalia were examined after clarification in clove oil and drawn with a camera lucida using an Olympus BH2 compound microscope. Incident light images were taken with a Leica M165C stereomicroscope, equipped with a Leica DFC290 digital camera. Measurements are given in millimeters. Format of descriptions follows Haddad *et al.* (2022) with leg spination as in Bosselaers & Jocqué (2000).

The following abbreviations are used in the descriptions: AER, anterior eye row; AL, abdomen length; ALE, anterior lateral eye; ALS, anterior lateral spinneret; AME, anterior median eye; AW, abdomen width; BG, Bennet's gland; BH, basal hematodocha; BU, bursa; CD, copulatory duct; CL, carapace length; CO, copulatory opening; CW, carapace width; DCD, distal copulatory duct; E, embolus; FD, fertilization duct; FVG, male palpal femur longitudinal ventral groove; Fu, fundus; MH, median hematodocha; MOQAW, anterior width of median ocular quadrangle; MOQL, median ocular quadrangle length; MOQPW, posterior width of median ocular quadrangle; PCD, proximal copulatory duct; PER, posterior eye row; PERW, posterior eye row width; PLE, posterior lateral eye; PLS, posterior lateral spinneret; plv, prolateral ventral spines of anterior legs; PME, posterior median eye; PMS, posterior median spinneret; rlv, retrolateral ventral spines of anterior legs; RCD, receptacle of copulatory duct; RPA, male palpal patella retrolateral apophysis; RTA, palpal tibia retrolateral apophysis; S1, primary spermatheca; S2, secondary spermatheca; St, subtegulum; TL, total length. Abbreviations in figures are detailed in legends.

For the phylogenetic analysis, we composed a dataset combining eight traditional target markers from the analysis of Wheeler *et al.* (2017) (12s, 16s, 18s, 28s, co1, H3), plus sequences from other sources and new co1 sequences for *P. paulae* (BOLD CORAR075, GenBank OR515542, MACN-Ar 30271) and *Trachelopachys sericeus* (BOLD SPDAR1264-15, GenBank OR515543, MACN-Ar 34546). Some markers were retrieved as bycatch from Sequence Read Archive (SRA) phylogenomic sequences processed by Martin Carboni (MACN); for this, first the mitochondri-

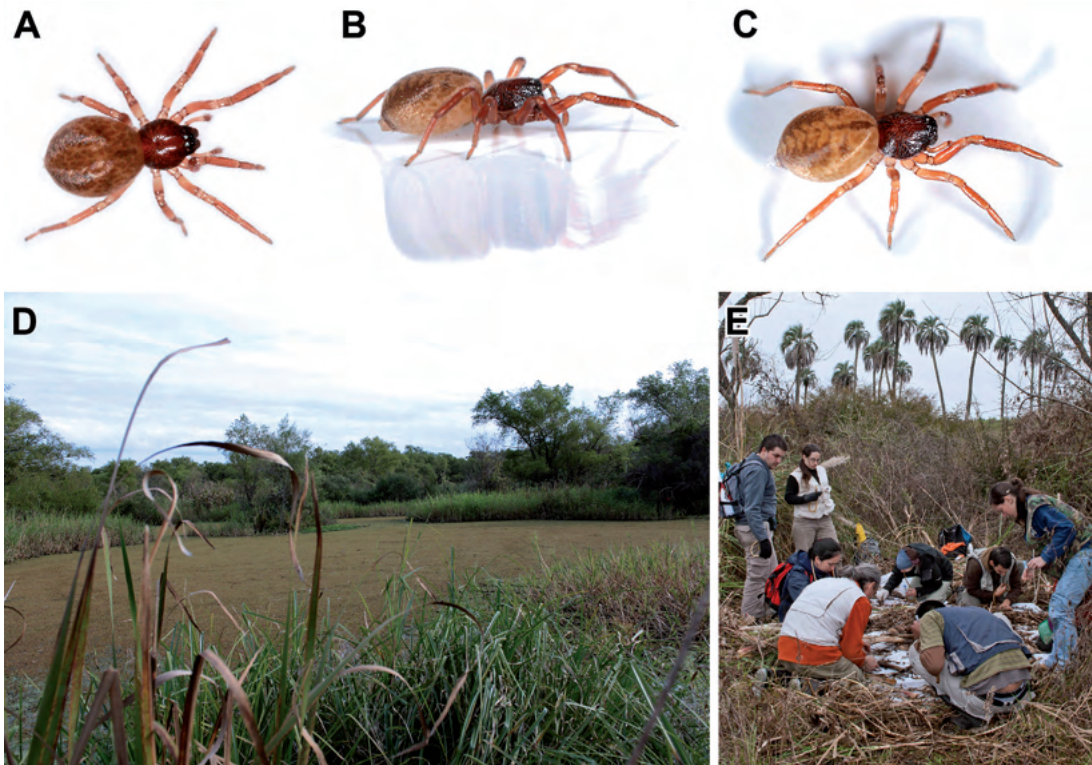


Fig. 1. Living specimens and habitat of *Paranita paulae*, new species. (A–C) female; (D) habitat in Parque Nacional Pre-Delta; (E) habitat in Parque Nacional El Palmar.

al genes were searched with mitofinder (Allio *et al.*, 2020), and the remaining genes, or also the mitochondrial ones if the first procedure failed, were found with BLAST (<https://blast.ncbi.nlm.nih.gov/Blast.cgi>), with the requested SRA as target. We used the morphological data accumulated in the datasets of Azevedo *et al.* (2022a) and Ramírez (2014). See Table S1 for sequence accession numbers and sources of data.

The analyses under maximum likelihood were made with IQ-TREE 2.2.0 (Minh *et al.*, 2020). Models for each target-gene were selected by Bayesian information criterion with ModelFinder (Kalyaanamoorthy *et al.*, 2017). The models selected for the sequence data were as follows: TIM2+F+G4 (12s and 16s), TNe+R2 (18s, *co1-2*, *h3-1*, *h3-2*), GTR+F+I+G4 (28s), GTR+F+I+G4 (*co1-1*), GTR+F+I+G4 (*co1-3*), GTR+F+I+G4 (*h3-3*). The morphological data was partitioned into two datasets, one with the unordered characters, another with the ordered ones, and analyzed with the Mk and Mk-ordered models, respectively, both with correction for

ascertainment bias for the absence of invariant characters. Prior to analysis, all invariant characters were removed, and polymorphic entries were replaced by missing entries. The branch support was estimated with 1000 rounds of ultrafast bootstrap (Hoang *et al.*, 2018).

The analyses under maximum parsimony were made with TNT v 1.6 (Goloboff & Catalano, 2016) under equal weights using an exact search of implicit enumeration. Branch support was measured with 1000 rounds of jackknifing, representing frequencies over the optimal tree. The synapomorphies common to all resolutions were calculated with TNT, over all the maximum likelihood bootstrapped trees compatible with the majority rule consensus with cutoff 70%.

The phylogenetic datasets and resulting trees are deposited in the repository of CONICET (<http://hdl.handle.net/11336/212403>) and in Zenodo (DOI: 10.5281/zenodo.8348985). The original images are deposited in CONICET (<http://hdl.handle.net/11336/212378>) and MorphBank (<https://www.morphbank.net/>, collection ID 799760).

TAXONOMY

Family Trachelidae Simon, 1897

Paranita new genus

LSID: urn:lsid:zoobank.org:act:1C03B372-A875-402C-88DC-19F271D966FF

Type species. *Paranita paulae*, new species.

Diagnosis. Species of the genus *Paranita* resemble those of *Orthobula* and *Capobula* in having pits on the carapace (Fig. 2A) and many pairs of large, ventral spines on tibia, metatarsus and tarsus I-II (Fig. 3C, D), and in lacking the ventral cusps (= short macrosetae) characteristic of many Trachelidae. *Paranita* species can be distinguished from species of those genera by lacking pits on the sternum, by having the male palp with the endites excavated externally, a long, coiled embolus, and a ventral femoral groove, instead of the femoral hook or projection found in *Orthobula* and *Capobula* (see Haddad *et al.*, 2022: fig. 26 and Haddad *et al.*, 2021: fig. 48, respectively).

Description. (Ultrastructural details are based on SEM images from *P. paulae*). Small spiders, 2.30–3.00 mm in length; carapace orange to reddish-brown, pear-shaped, broadest at coxae II, without fovea (Fig. 2A); posterior margin slightly concave to straight; surface shiny, profusely covered with deep pits, at least on lateral areas, each pit an elongate depression (Fig. 2G); surface sparsely covered with fine setae (Fig. 2G). All eyes surrounded by black rings, weaker around PME; AER procurved in anterior view, straight in dorsal view (Figs. 2B, C); AME slightly larger than ALE; AME separated by approximately $\frac{3}{4}$ their diameter, slightly closer to ALE; PER nearly straight in dorsal view, PME slightly irregular and silvery, with tapeta disposed orthogonally, all other eyes round; PME and PLE similar in diameter; median ocular quadrangle about as wide anteriorly as posteriorly to slightly narrower anteriorly, length and posterior width approximately equal. Chilum indistinct, a single median sclerite; cheliceral promargin with three teeth, separated by approximately their basal width, proximal tooth smallest; retromargin with two subequal teeth, set close together (Fig. 2H–K); cheliceral escort setae present on both margins (Fig. 2H, J); fang with distinct serrula; endites convergent, notched laterally (Fig. 2D), with distinct serrula (Fig. 2F); dense maxillary hair tuft on mesal margins (Fig. 2F); labium tra-

pezoidal, slightly wider than long, concave distally. Pleural bars sclerotised, fused to each other, separated from carapace; sternum shield-shaped, longer than broad, surface smooth without pits, sparsely covered in thin setae (Fig. 2D); precoxal triangles present, fused to sternum. Female palpal tarsus slightly thickened, claw simple and sharp, nearly straight (Fig. 3A, B). Leg formula 4123 or 1423, legs I and IV very similar in length; leg cuticle fingerprint-like to smooth, sparsely covered in long fine setae, without scales; femora I with mesal convex curvature, all femora constricted proximally; legs I–II with long series of strong ventral spines on tibia, metatarsus and tarsus (Fig. 3C, D), each spine with lobed socket and a flat tenent surface at the tip (Fig. 3D–H); metatarsi with single line of trichobothria, distal one very long and bent at angle (Fig. 4G, H), metatarsi III and IV with ventral preening comb at distal end (Fig. 4D); tarsi with few trichobothria in two rows (Fig. 4A); trichobothria with sunken distal plate, hood with about four ridges (Fig. 4F); tarsal organ oval, very slightly elevated from integument, surface fingerprinted, opening oval and distally placed (Fig. 4A, E). Paired tarsal claws short, with about four teeth, claw tufts made of about 8 tenent setae on each side, with wide folding bases, a tooth from the claw base (claw tuft clasper) locking on a claw tuft seta (Fig. 5); claw lever with wide lateral wings at the sides, appressed against the base of a claw tuft seta (Fig. 5C, G). Abdomen oval, larger in females than males, without dorsal scutum; dorsum with sparse fine setae; abdominal background color cream, with dark brown markings on cardiac area, posterior dorsal area and at side of spinnerets' insertion, with pale cream dorsal chevrons; venter pale, without post-epigastric sclerites or any sclerotized area. Spinnerets (details observed in *P. paulae* only): female (Fig. 6): colulus as a hairy patch; ALS with one major ampullate gland spigot and a nubbin, and 5–6 piriform gland spigots; anterior region of PMS with two minor ampullate gland spigots and 13 aciniform gland spigots, posterior region with four large cylindrical gland spigots; PLS with two large cylindrical gland spigots and 11–12 aciniform gland spigots, and a modified spigot on the posterior lateral margin; male spinnerets (Fig. 7): ALS with one major ampullate gland spigot and a nubbin, and 5–6 piriform gland spigots; PMS with two minor ampullate gland spigots and 8 aciniform gland spigots; PLS with 10 aciniform gland spigots and a modified spigot on the center; epiandrium without spigots (Fig.

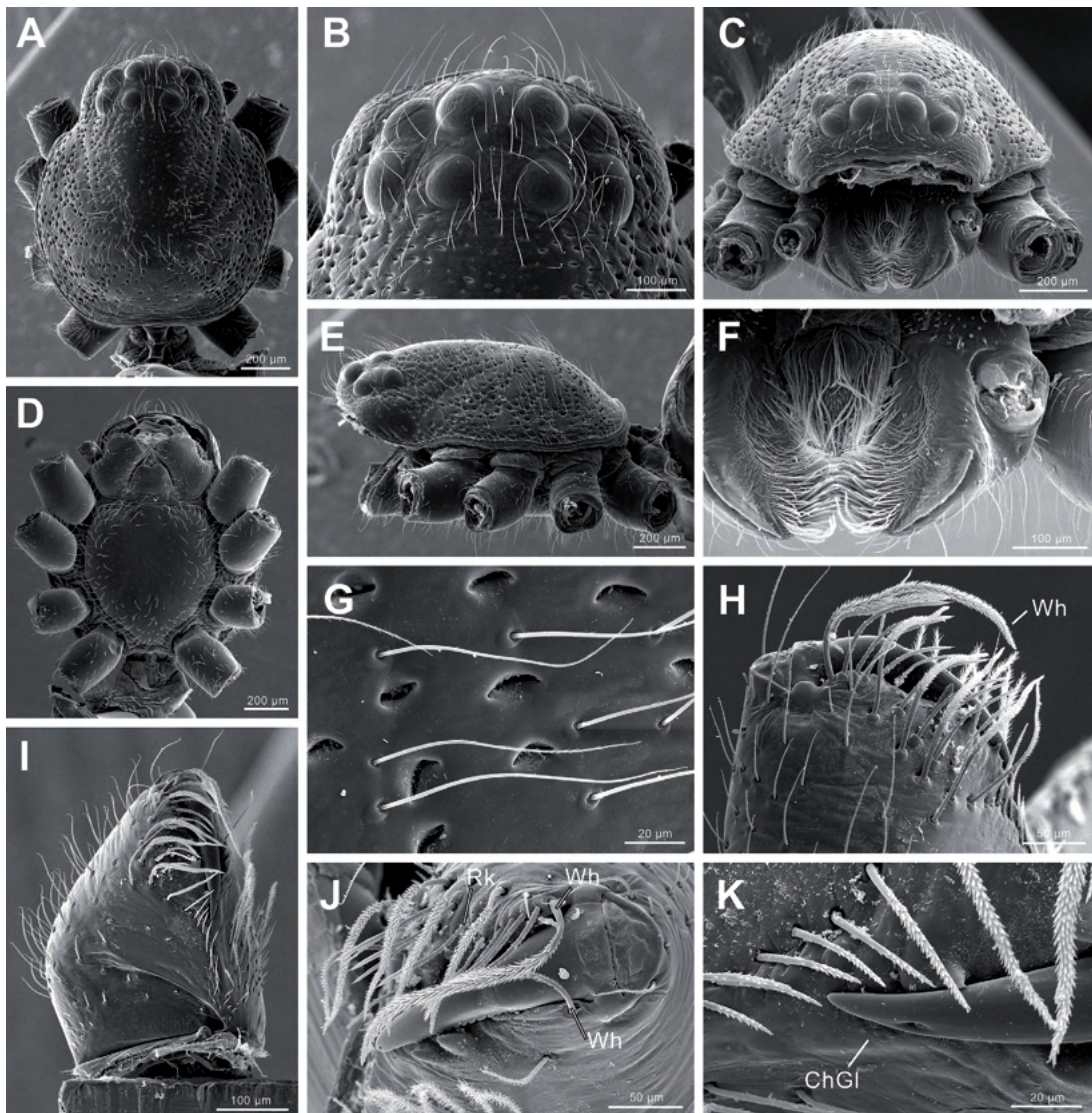


Fig. 2. *Paranita paulae*, new species, structures of female prosoma (MACN-Ar 43421). (A) carapace, dorsal view; (B) same, detail of eyes; (C) prosoma, anterior view; (D) same, ventral view; (E) same, lateral view; (F) endites and labium, anterior view; (G) detail of pores on carapace; (H) left chelicera, anterior view; (I) same, mesal view; (J) same, ventral view; (K) same, detail of venom outlet and cheliceral gland. Abbreviations: ChGl, cheliceral gland, Rk, promarginal rake seta, Wh, cheliceral whisker seta.

7E). Respiratory system consisting of anterior book lungs, with spiracle unmodified (Fig. 7F), and four simple tracheae limited to opisthosoma, tracheal spiracle close to the spinnerets (Fig. 6A). Male palpal femur with longitudinal ventral groove (FVG; Fig. 8B, 9A); endite excavated externally (Fig. 9D), palpal patella with (Fig. 8C) or without retrolateral apophysis (RPA); palpal tibia with elongate retrolateral apophysis (RTA) curving upwards (Fig. 8C); cymbium with an api-

cal, ventral group of thick setae; tegulum simple, without median apophysis or conductor; embolus filiform, making a clockwise circle as seen in the left palp in retrolateral view; the expanded bulb (Fig. 9E, F) shows a large basal hematodocha (BH), small subtegulum (St), and the median hematodocha (MH) continuous with the BH, spermophore gradually tapering from fundus (Fu) to tip of embolus (E) without expansions or constrictions. Female genitalia (Figs 9G, 10) with

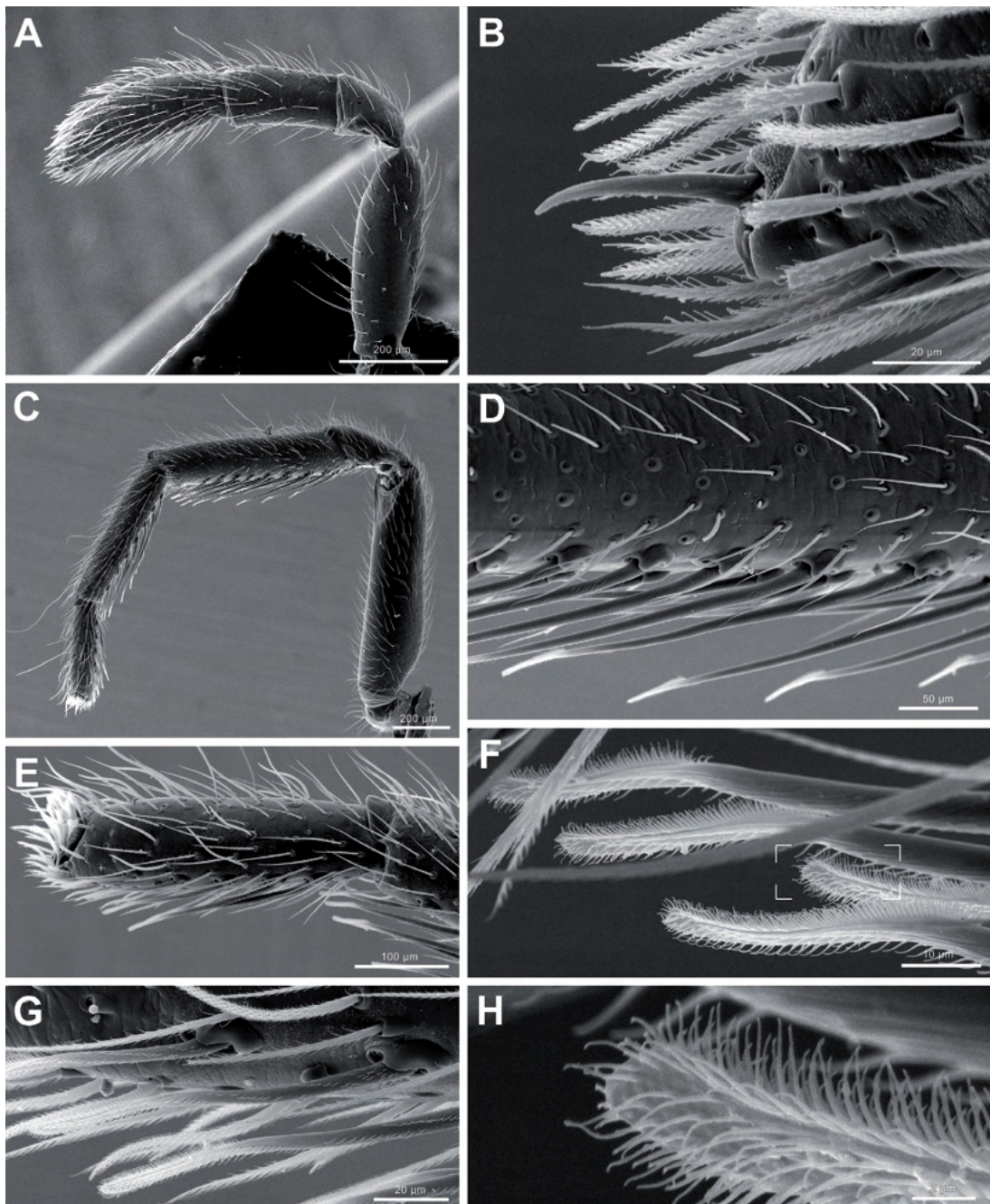


Fig. 3. *Paranita paulae*, new species, structures of female palp and leg I (MACN-Ar 43421). (A) left palp, retrolateral view; (B) same, detail of palpal claw; (C) left leg I, retrolateral view; (D) same, detail of ventral tibial macrosetae; (E) detail of tarsus I; (F) detail of metatarsal macrosetae showing apical tenent surface (see closeup of marked area in H); (G) detail of tarsal macrosetae; (H) detail of tenent tip of metatarsal macroseta, as marked in F.

small, paired copulatory openings (CO) positioned centrally or slightly posteriorly on epigynal plate (Fig. 10D), copulatory duct (CD) leading anteriorly to the secondary spermatheca (S2) in

the form of a large anterior receptacle with sparse gland ducts (Fig. 10B, C), from there the distal part of the CD leads to a second receptacle, an expanded part of the CD (the receptacle of the

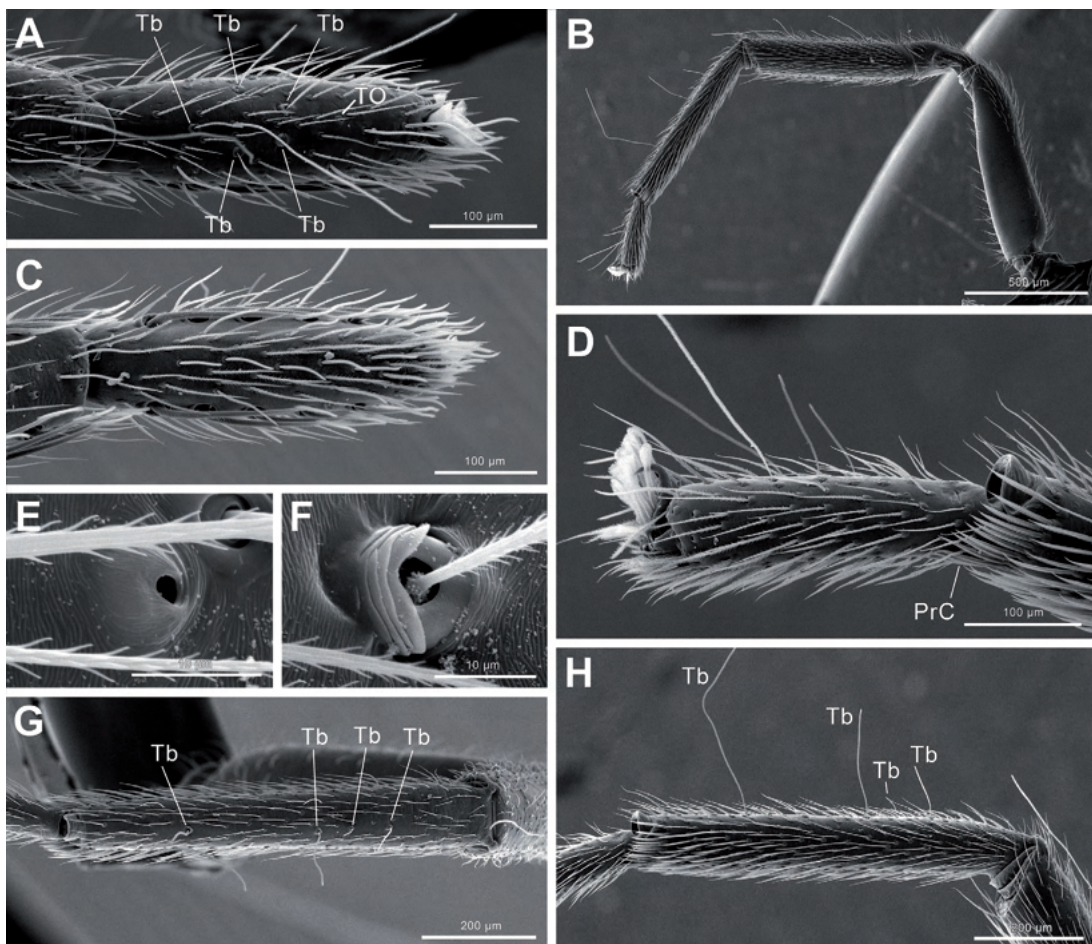


Fig. 4. *Paranita paulae*, new species, structures of female legs I and IV (MACN-Ar 43421). (A) left tarsus I, dorsal view; (B) left leg IV, retrolateral view; (C) left tarsus I, ventral view; (D) left tarsus IV, retrolateral view; (E) tarsal organ I; (F) trichobothria on tarsus I; (G) metatarsus IV, dorsal view; (H) same, retrolateral view. Abbreviations: PrC, preening comb; Tb, trichobothria; TO, tarsal organ.

CD), and finally leading to the third receptacle, the primary spermatheca (S1), from where the fertilization duct (FD) arises (Fig. 10A, B, E).

Etymology. The generic name is a free combination of letters, derived from the Paraná River and an ending that sounds diminutive in Spanish. Gender is feminine.

Paranita paulae new species (Figs. 1–14, 16)

LSID: urn:lsid:zoobank.org:act:6047685F-7AE1-4856-B91B-FE130CA30C7B

Trachelidae ARG. Ramírez, 2014: 390.

Cf. *Orthobula* sp. Azevedo et al., 2022a: fig. 3.

Diagnosis. Males of *P. paulae* can be easily distinguished from those of *Paranita inesae* sp. n. by the flat copulatory bulb a with long coiling embolus (Figs. 9A, 11I), while in *P. inesae* the bulb is nearly spherical, and the embolus is much shorter. The females can be distinguished by the very long, coiled copulatory ducts and smaller secondary spermatheca, as well as the copulatory openings in the posterior part of the epigynal plate (Fig. 9G, 12F).

Description. Male. (Holotype). Measurements: CL 1.12, CW 0.96, AL 1.30, AW 0.94, TL 2.40, PERW 0.44, MOQAW 0.20, MOQPW 0.24, MOQL 0.22. Length of leg segments: I 0.80 + 0.38 + 0.64 + 0.54 + 0.32 = 2.68; II 0.72 + 0.32 + 0.64 + 0.50 + 0.28 = 2.46; III 0.54 + 0.30 + 0.34 + 0.44 + 0.24 = 1.86; IV 0.76 + 0.28 + 0.60 + 0.68 = 2.32.

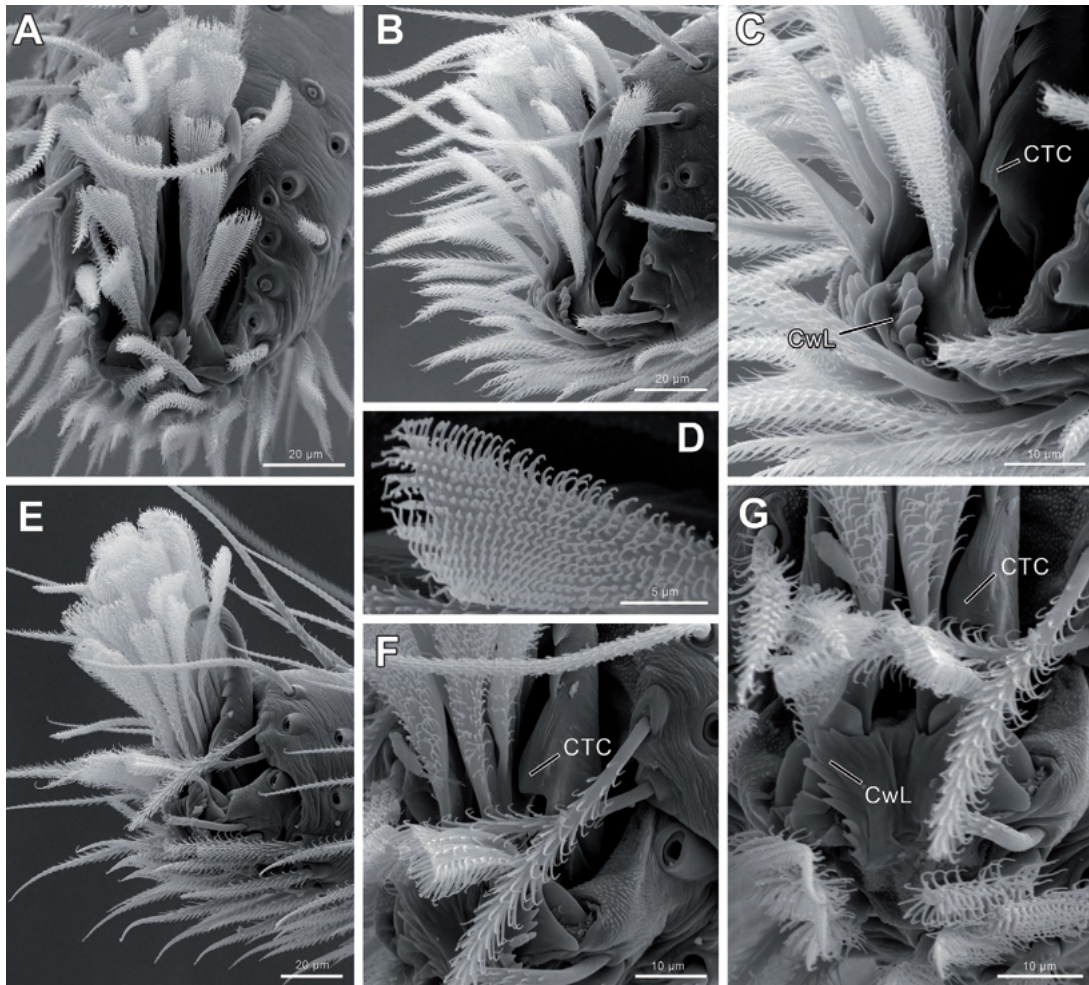


Fig. 5. *Paranita paulae*, new species, structures of female claws and claw tufts I and IV (MACN-Ar 43421). (A) left claws and claw tufts I, apical view; (B) same, retrolateral view; (C) same, detail of bases of claw tuft and claws; (D) detail of tenent surface of claw tuft seta on tarsus I; (E) left claws and claw tufts IV, retrolateral view; (F) same, detail of bases of claw tuft and claws; (G) same, apical view. Abbreviations: CTC, claw tuft clasper; CwL, claw lever.

+ 0.24 = 2.56. Carapace profusely pitted, pits covering almost entire surface, except two small smooth areas on the posterior part of cephalic area and on anterior part of thoracic region (Fig. 2D, 11D). Color (Fig. 11): carapace deep orange-brown; chelicerae orange-brown; endites slightly paler than chelicerae, cream distally; labium brown; sternum smooth, uniform light orange, slightly darker at the margins; palps and legs light brown, except the coxae, cream; abdomen white dorsally, with an anteromedian elongate grey patch and two small anterolateral ones, two posterolateral dark grey bands with irregular ventral border and with more or less triangular extensions pointing to dorsum, the more caudal markings almost touching at dorsal midline, ex-

panding ventrally as an open ring around spinnerets; venter whitish, spinnerets whitish. Leg spination: femora and patellae spineless; tibiae: I plv 8/9 rlv 8, II plv 7 rlv 5; metatarsi: I plv 7 rlv 7, II plv 6 rlv 6; tarsi: I plv 3 rlv 4, II plv 3 rlv 2. Legs III and IV spineless, but with apical combs on metatarsi. Palp (Fig. 8, 9A-E): femur with ventral longitudinal furrow, patella with ventral retrolateral pointed apophysis; tibia relatively short, with long, sword-shaped retrolateral apophysis curving upwards; bulb large, discoidal, embolus very long, mostly filiform, encircling tegulum twice, with a serrated margin at the proximal part.

Female. (Paratype, MACN-Ar 43423). Measurements: CL 1.22, CW 1.10, AL 1.64, AW 1.18,

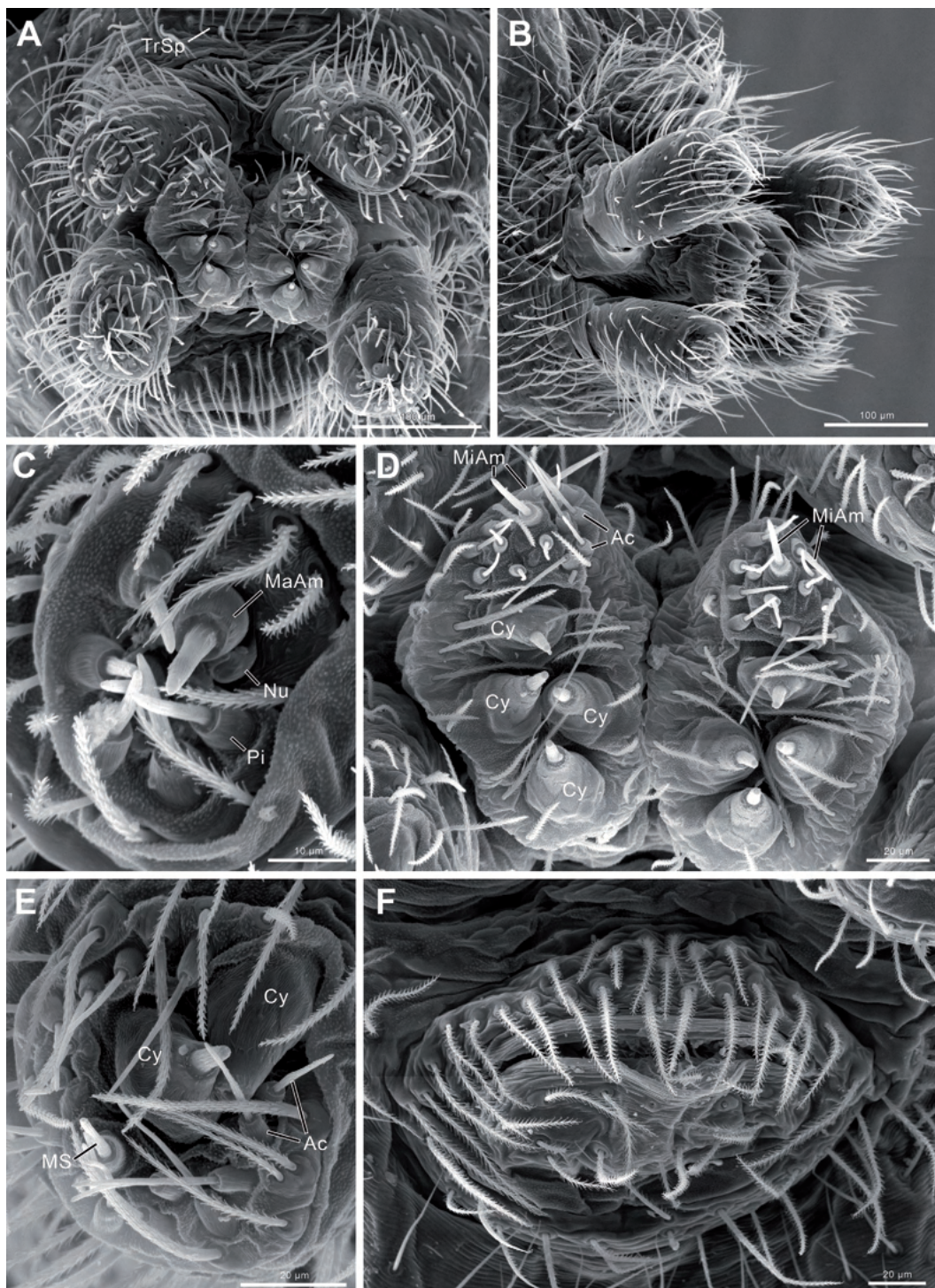


Fig. 6. *Paranita paulae*, new species, female spinnerets and anal tubercle (MACN-Ar 43421). (A) spinnerets, ventral view; (B) same, lateral view; (C) right anterior lateral spinneret; (D) posterior median spinnerets; (E) right posterior lateral spinneret; (F) anal tubercle. Abbreviations: Ac, aciniform gland spigot; Cy, cylindrical gland spigot; MaAm, major ampullate gland spigot; MiAm, minor ampullate gland spigot; MS, modified PLS spigot; Nu, nubbin of ampullate gland spigot; Pi, piriform gland spigot; TrSp, tracheal spiracle.

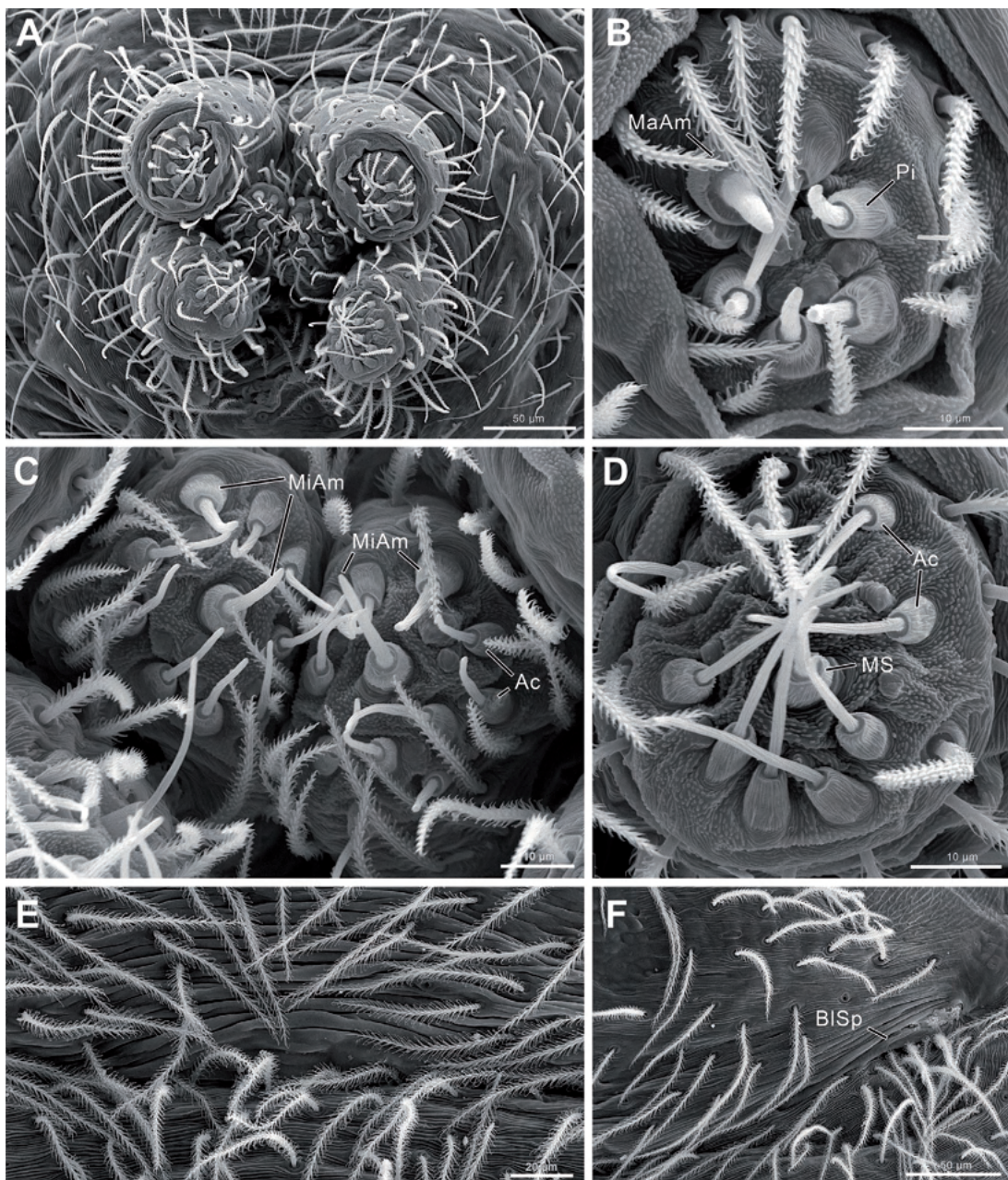


Fig. 7. *Paranita paulae*, new species, male spinnerets and epigastric area (MACN-Ar 43421). (A) spinnerets, ventral view; (B) left anterior lateral spinneret; (C) posterior median spinnerets; (D) left posterior lateral spinneret; (E) epiandrium; (F) book lung spiracle. Abbreviations: Ac, aciniform gland spigot; BlSp, book lung spiracle; MaAm, major ampullate gland spigot; MiAm, minor ampullate gland spigot; MS, modified PLS spigot; Pi, piriform gland spigot.

TL 2.76, PERW 0.52, MOQAW 0.20, MOQPW 0.24, MOQL 0.22. Length of leg segments: I $0.90 + 0.42 + 0.76 + 0.60 + 0.32 = 3.00$; II $0.80 + 0.38 + 0.62 + 0.54 + 0.32 = 2.66$; III $0.64 + 0.34 + 0.40 + 0.52 + 0.24 = 2.14$; IV $0.90 + 0.36 +$

$0.74 + 0.82 + 0.32 = 3.14$. Colour and sculpturing (Fig. 12) as in male, but the anterolateral abdominal patches more posteriorly located, and lateral markings touching at dorsally in posterior third. Leg supination (Fig. 12G, H): femora

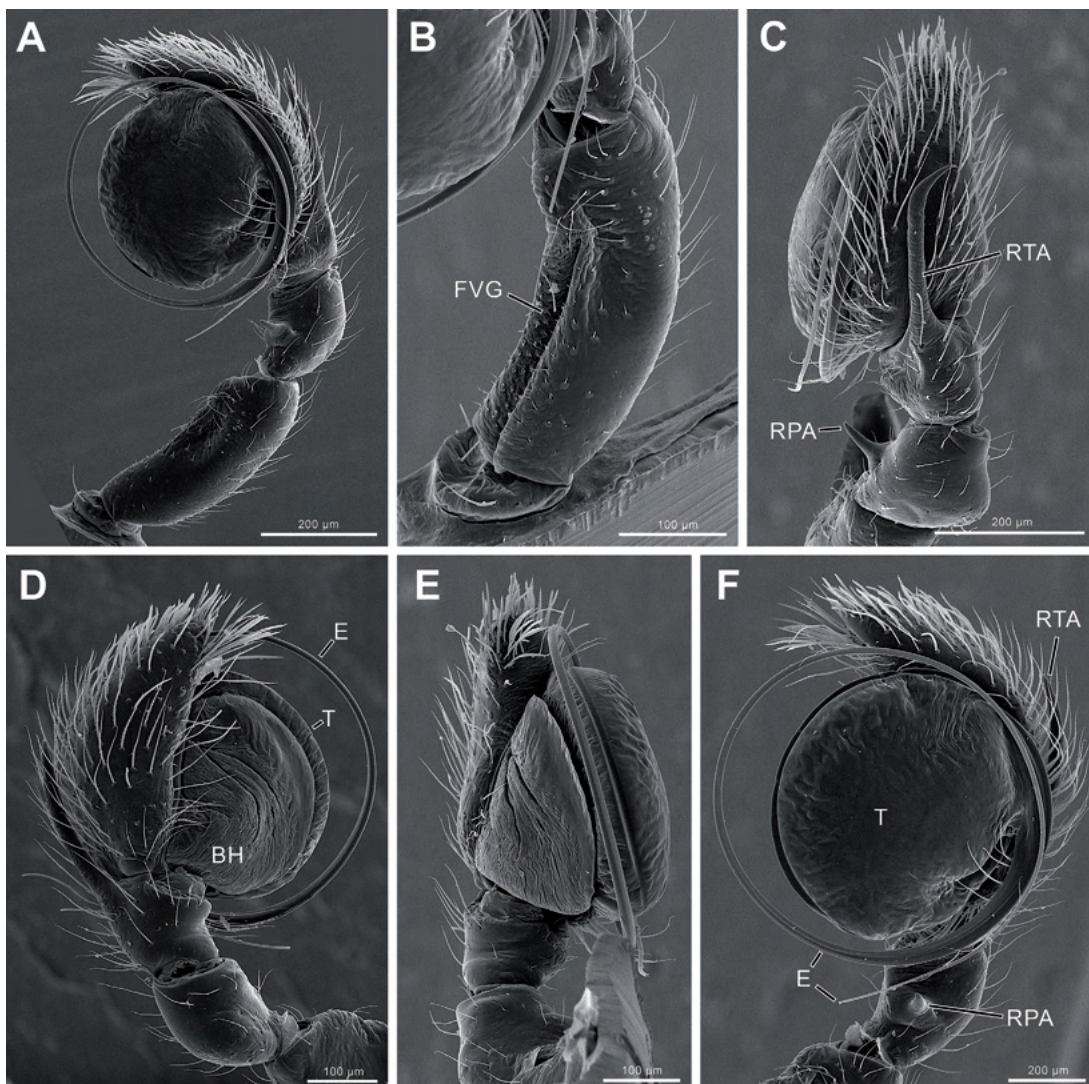


Fig. 8. *Paranita paulae*, new species, left male palp (MACN-Ar 43421). (A) retrolateral view; (B) femur, retrolateral view; (C) dorsal view; (D) prolateral view; (E) ventral view; (F) detail of retrolateral view. Abbreviations: BH, basal hematodocha; E, embolus; FVG, femoral ventral groove; RPA, retrolateral patellar apophysis; RTA, retrolateral tibial apophysis; T, tegulum.

and patellae spineless; tibiae: I plv 10, rlv 9 (with two rows of four smaller spines between plv and rlv), II plv 8, rlv 7 (with one row of four smaller spines between plv and rlv); metatarsi: I plv 7 rlv 7, II plv 7 rlv 6; tarsi: I plv 6 rlv 5, II plv 6 rlv 3. Legs III and IV spineless, but with apical combs on metatarsi. Epigynal plate pale orange, with internal structures visible through cuticle: copulatory openings oval, small, located posteriorly (Fig. 12F). Internal genitalia (Figs. 9G, 10) consisting of three paired receptacles connected by coiling copulatory duct; membranous proximal

copulatory duct (PCD) leads to oval secondary spermatheca (S2), from there the more sclerotized distal copulatory duct (DCD) leads to oval receptacle of copulatory duct (RCD), and finally to primary spermatheca (S1); Bennet's gland (BG) discharging at side of S2.

Type material. Holotype male from Argentina. Buenos Aires Province: Zárate Dept.: Isla Talavera, 2 km E Zárate, [ca. S34.1020833° W58.980475°], 3 Nov. 1996, M. J. Ramírez (MACN-Ar 43425, voucher CJG-2065). Paratypes: same data as the holotype, 1♂, 1♀ (MACN-Ar 43424, female

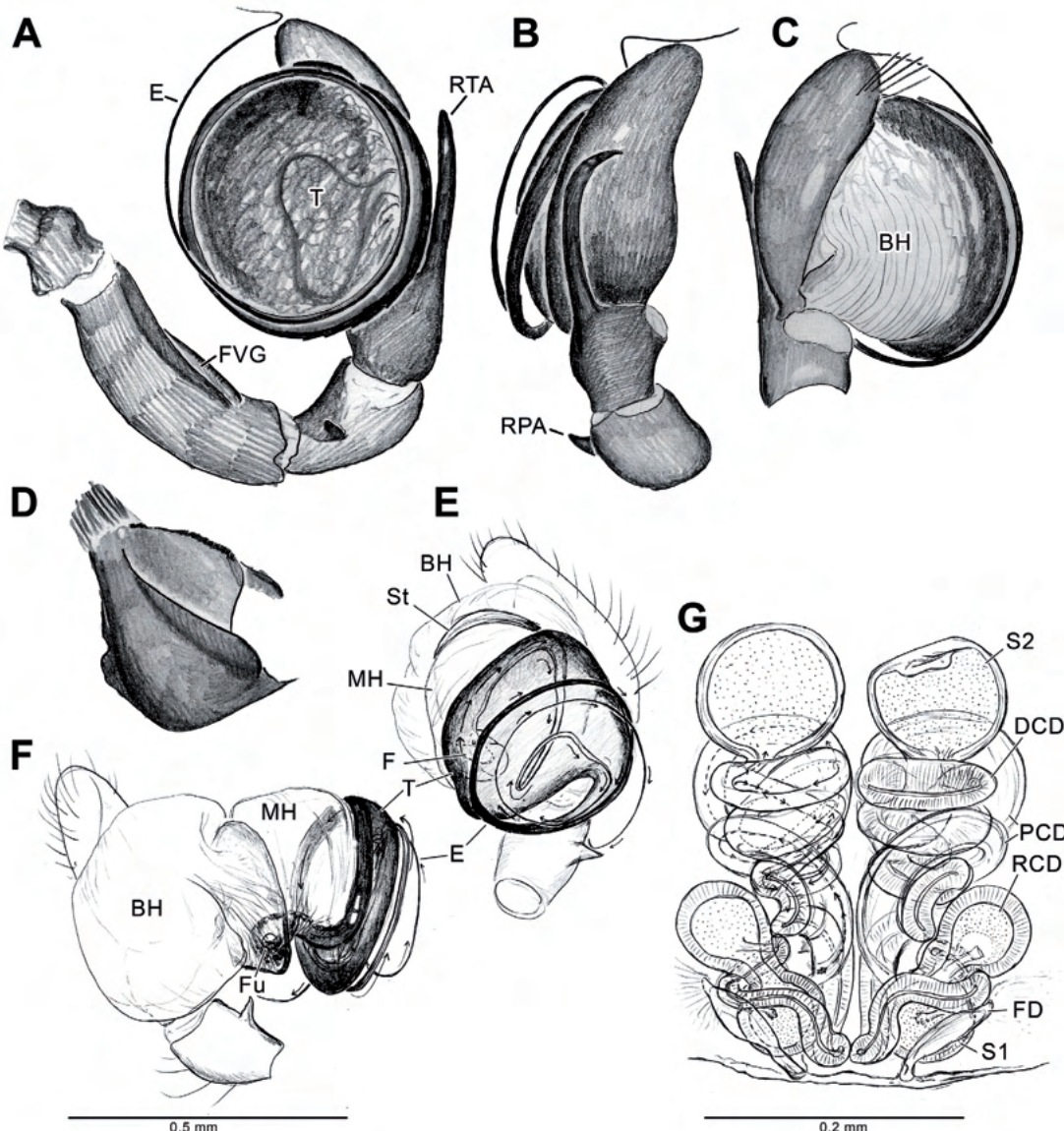


Fig. 9. *Paranita paulae*, new species, genitalia. (A–D) paratype male (MACN-Ar 43424), (A) left male palp, retrolateral view; (B) same, dorsal view; (C) same prolateral view; (D) left male endite, ventral view. (E–F) paratype male (MACN-Ar 43423), (E) left male palp, expanded, ventral view; (F) same, prolateral view. (G) female spermathecae of the female paratype (MACN-Ar 43424), dorsal view. Abbreviations: DCD, distal copulatory duct; E, embolus; FD, fertilization duct; Fu, fundus; FVG, femoral ventral groove; PCD, proximal copulatory duct; RCD, receptacle on copulatory duct; RPA, retrolateral patellar apophysis; RTA, retrolateral tibial apophysis; S1, primary spermatheca; S2, secondary spermatheca (=accessory bulb); St, subtegulum; T, tegulum.

voucher ARAMR000926, CJG-488, CJG-2066); 1♂, 1♀ (MACN-Ar 43423, female voucher ARA-MR000925, CJG-487, male voucher ARA-MR000924, CJG-485, 486, 493); 1♂, 7♀ (MACN-Ar 43422), 1♂, 1♀ (MLP); Corrientes Province: San Miguel, Parque Nacional Iberá, Portal San Nicolás, 28°10'S, 57°26'W, 16 May. 2022, Ávalos,

Achitte, Nadal, Mandieta, 1♀ (CARTROUNNE 9776).

Other material examined. Buenos Aires Province: Same data as the types, 1♂, 1♀ (MACN-Ar 43421, voucher MJR-1291-1299); same department: La Palmas, [ca. S34.0691667° W59.1511111°], Jun. 1982, M. J. Ramírez, 1♀

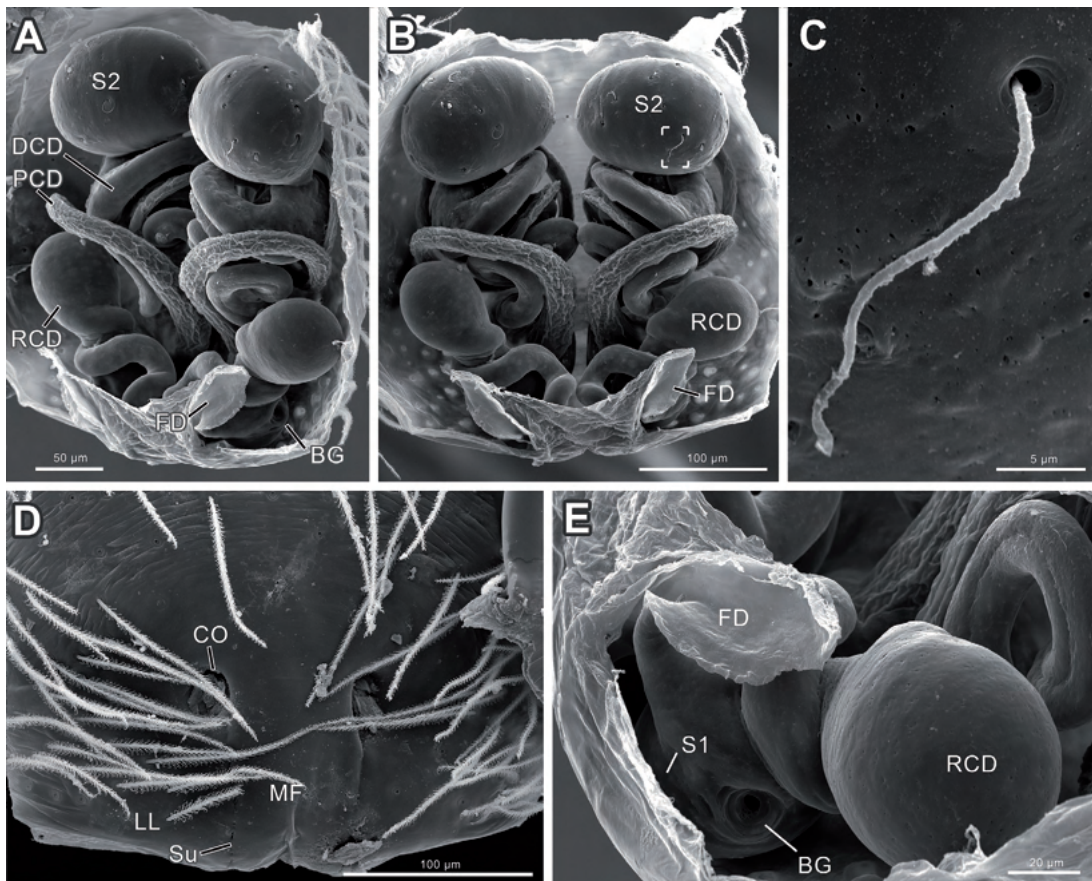


Fig. 10. *Paranita paulae*, new species, female genitalia (MACN-Ar 43421). (A) spermathecae, ventrolateral view; (B) same, ventral view surface (see closeup of marked area in C); (C) detail of gland duct on S2, as marked on B; (D) epigyne, ventral view; (E) left spermatheca, ventrolateral view. Abbreviations: BG, Bennett's gland; DCD, distal copulatory duct; FD, fertilization duct; PCD, proximal copulatory duct; RCD, receptacle on copulatory duct; S1, primary spermatheca; S2, secondary spermatheca (=accessory bulb).

(MACN-Ar 17270); Campana Dept.: Reserva Natural Otamendi (currently Parque Nacional Cielo de los Pantanos): Estación Río Luján [ca. S34.278017, W58.890346], 5 Oct. 1993, M. Ramírez and A. Pérez González, 1♂, 1♀ (MACN-Ar 17262); Tigre Dept.: Benavídez [ca. S34.4115721, W58.6899278], 26 Sep. 1982, P. Goloboff and M. Ramírez 2♀ (MACN-Ar 43417); Delta del Río Paraná, Río San Antonio [ca. S34.3877528°, W58.5356666°], May 1942, dad. Sr. Monrós, 1♀ (MACN-Ar 42886, ex MACN-Ar 20927); Delta del Río Paraná, Río Luján y Arroyo Guayracá [S34.3661889°, W58.6601305°], Jun. 1982, M. Ramírez, 2♀ (MACN-Ar 17267); Reserva Hotel "Amarran Sancho", S34.36377°, W58.59774° (+/-500 m), elev. 7 m, 11–12 Apr. 2015, pajonal, C. J. Grismado, L. N. Piacentini, N. López Carrión, D. Proud and J. Varano, col-

lecta manual, 1♀ (MACN-Ar 34322, voucher CJG 3368), same data, under *Cortaderia selloana*, 1♀ (MACN-Ar 34660, voucher CJG 3390); Tigre [ca. S34.4115721, W58.6899278], no date, J. Viana, 2♀, 1 immature (MACN-Ar 43414); Delta del Río Paraná, no precise locality, 11 Jul. 1949, J. Viana, 2♂♂, 1♀ (MACN-Ar 2949); La Plata Dept.: Isla Martín García [ca. S34.18522654°, W58.25126161°], 1940, J. Viana, 1♂, 1 immature (MACN-Ar 43415); Azul Dept.: Sierras de Azul, [ca. S34.06916667° W59.1511111°], 1–2 Oct. 1983, A. Zanetic and P. A. Goloboff, 1♀ (MACN-Ar 17271). Entre Ríos Province: Parque Nacional Predelta, isla frente a seccional, 6 km S Diamante, S32.12140° W 60.63528° (+/-50 m), elev. 10 m, 1 May 2013, bosque de alisos y enredaderas, golpeteo de follaje, M. J. Ramírez, L. N. Piacentini, M. E. González, A. Laborda and S. Aisen,

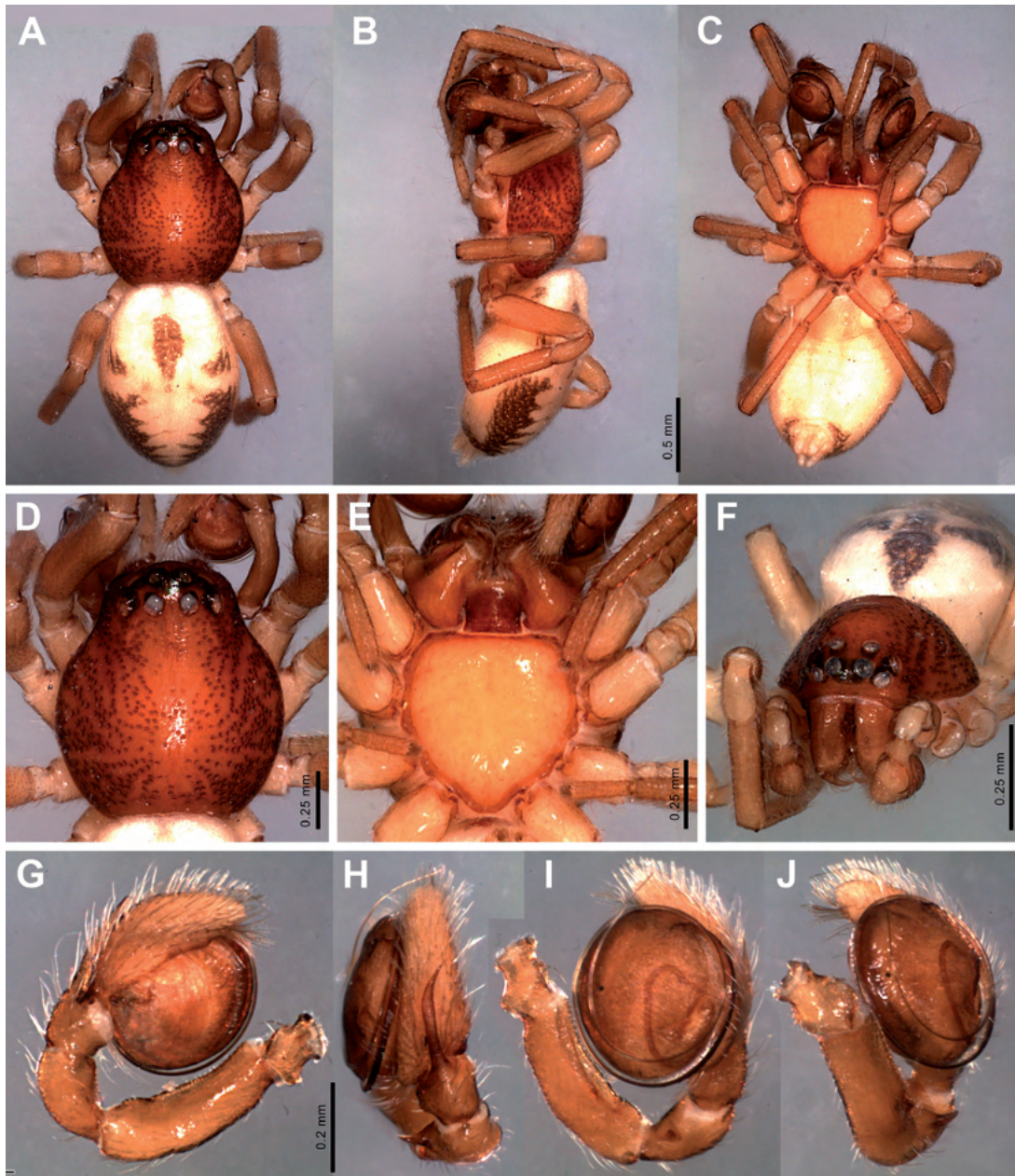


Fig. 11. *Paranita paulae*, new species, holotype male (MACN-Ar 43425). (A) habitus dorsal; (B) same, lateral; (C) same ventral; (D) carapace, dorsal view; (E) prosoma, ventral view; (F) prosoma, anterior view; (G) left male palp, prolateral view; (H) same, dorsal view; (I) same, retrolateral view; (J) same, ventral-retrolateral view.

1♀ (MACN-Ar 30268); same locality and collectors, bañado cerca de entrada, 6 km S Diamante, S32.12194° W 60.62996° (+-20m), elev. 10 m, 30 Apr. 2013, bañado en laguna, colecta manual, 1♂ (MACN-Ar 30271, co1 sequenced CORAR075), 1♀ (MACN-Ar 30272); Uruguay Dept.: Ruta Nac. 14, 7 km E Concepción del Uruguay, S32.483128°

W58.308484° (+-50m), elev. 26 m, 8 Aug. 2011, borde de ruta, *Eryngium* y pastos, M. J. Ramírez y equipo MACN-Ar, 1♀ (MACN-Ar 33414); Colón Dept.: Parque Nacional El Palmar, S31.88484° W58.23930° (+-10 m), elev. 25 m, 7 Aug. 2011, pastizal cerca de bañado, en macollo de pastos, M. J. Ramírez y equipo MACN-Ar, 1♀ (MACN-Ar

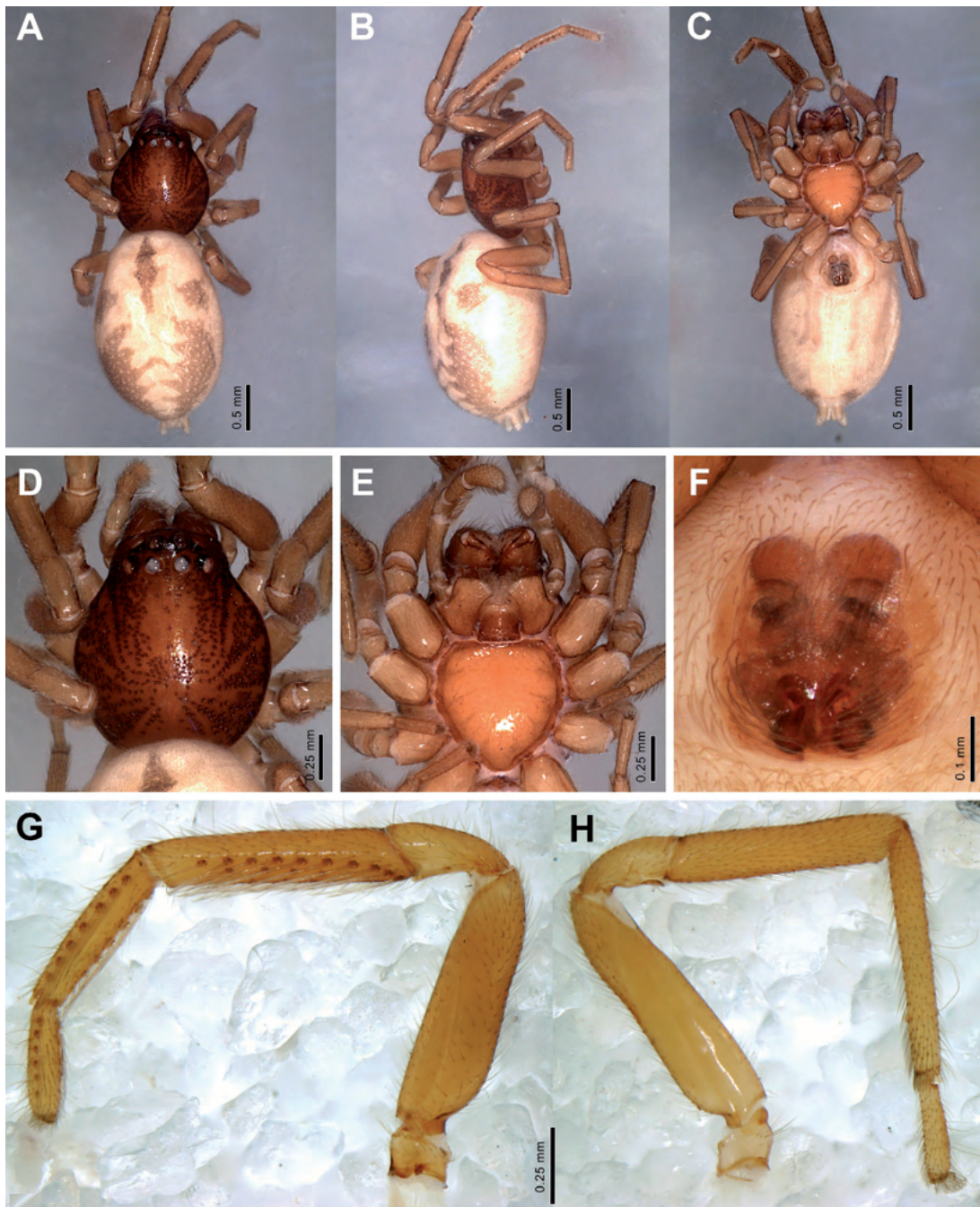


Fig. 12. *Paranita paulae*, new species, female paratypes. (A–E) MACN-Ar 43424, (A) habitus dorsal; (B) same, lateral; (C) same ventral; (D) carapace, dorsal view; (E) prosoma, ventral view. (F–H) MACN-Ar 43423, (F) epigyne, ventral view; (G) left leg I, retrolateral view; (H) left leg IV, prolateral view.

38414), 1♀ (MACN-Ar 33166); 1♂, 1♀ (MACN-Ar 33179); same locality and collectors, S31.86539° W58.24008° (+-10 m), elev. 28 m, 7–8 Aug. 2011, pastizal anegable, en macollo de pastos y *Corta-*

deria selliana, 1♀ (MACN-Ar 32759), 1♀ (MACN-Ar 32750), 1♀ (MACN-Ar 32751), 1♀ (MACN-Ar 32799), 1♀ (MACN-Ar 32839), 1♀ (MACN-Ar 32833), 1♂, 1♀ (MACN-Ar 32802); 1♂, 2♀ (MACN-

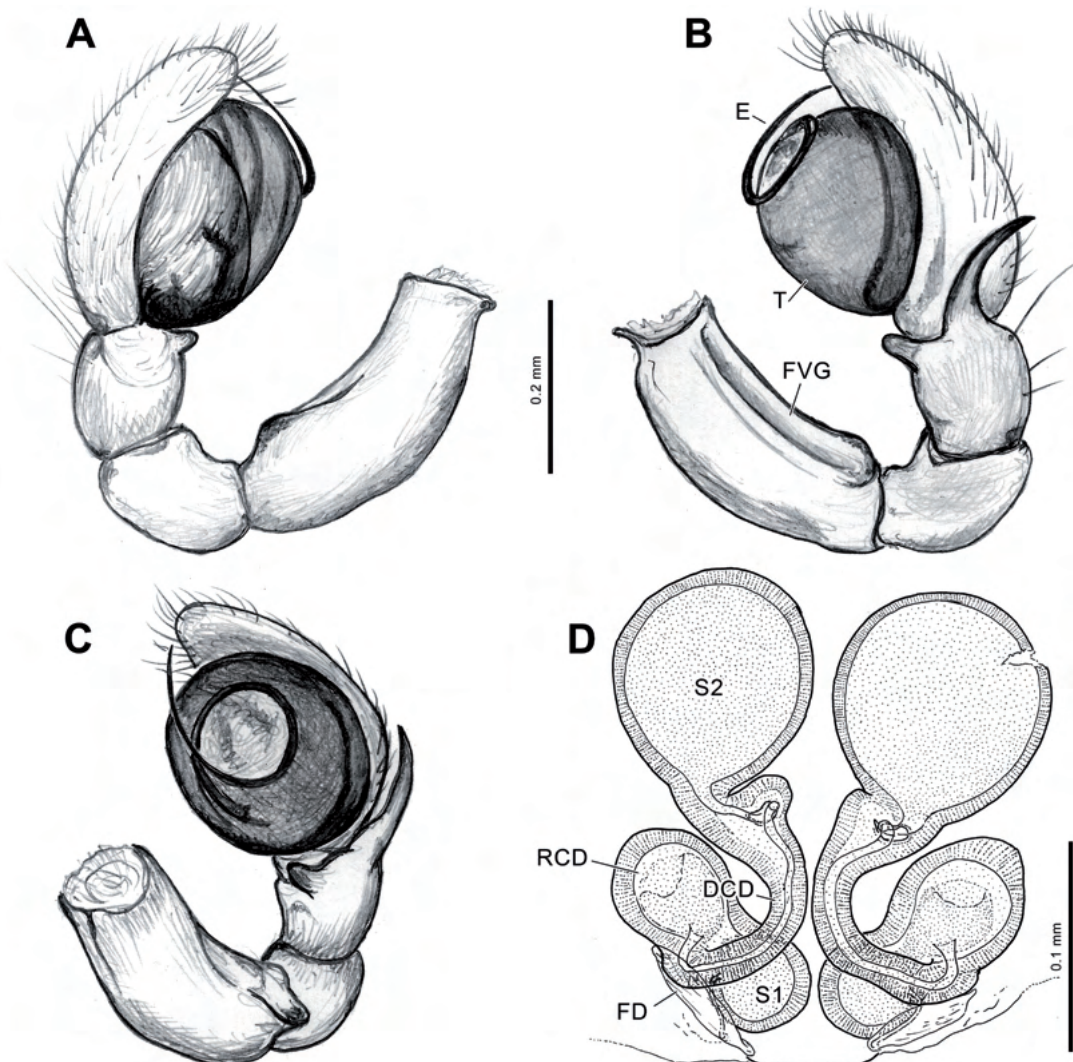


Fig. 13. *Paranita inesae*, new species, genitalia. (A–C) holotype male (MACN-Ar 43412), (A) left male palp, prolateral view; (B) same, retrolateral view; (C) same, ventral view; (D) spermathecae of female (MACN-Ar 43413), dorsal view. Abbreviations: DCD, distal copulatory duct; E, embolus; FD, fertilization duct; FVG, femoral ventral groove; RCD, receptacle on copulatory duct; S1, primary spermatheca; S2, secondary spermatheca (=accessory bulb); T, tegulum.

-Ar 32888). Corrientes Province: San Miguel, Estancia San Juan Poriajú, Iberá, 27°41'S, 57°11'W, 20 Nov. 2013, forest, litter, G. Ávalos, 1♂ (CARTROUNNE 9778); Santo Tomé Galazar, Iberá, 28°6'S, 56°41'W, 23 Nov. 2012. G. Ávalos, 2♀ (CARTROUNNE 9779). Misiones Province: Concepción Dept.: Santa María [ca. S27.9011111°, W55.4069444°], no date, J. Viana, 1♀ (MACN-Ar 17265), same province, no precise locality, May 1960, J. Viana col. 1♀ (MACN-Ar 43416).

Etymology. The specific name is in honor of Paula Magariños, spouse of the first author, in homage of her love of scary little critters that are

nice on a closer look, like this spider species.

Distribution. Wetlands and grasslands in the Paraná and Uruguay River basins in Argentina, in Buenos Aires, Entre Ríos, Corrientes and Misiones provinces. One isolated record in Sierras de Azul, south of Buenos Aires Province may indicate a wider distribution in the province.

***Paranita inesae* new species
(Figs. 13–16)**

LSID: urn:lsid:zoobank.org:act:E3E557B-2-0045-4FB8-950D-A4AB956DE08F

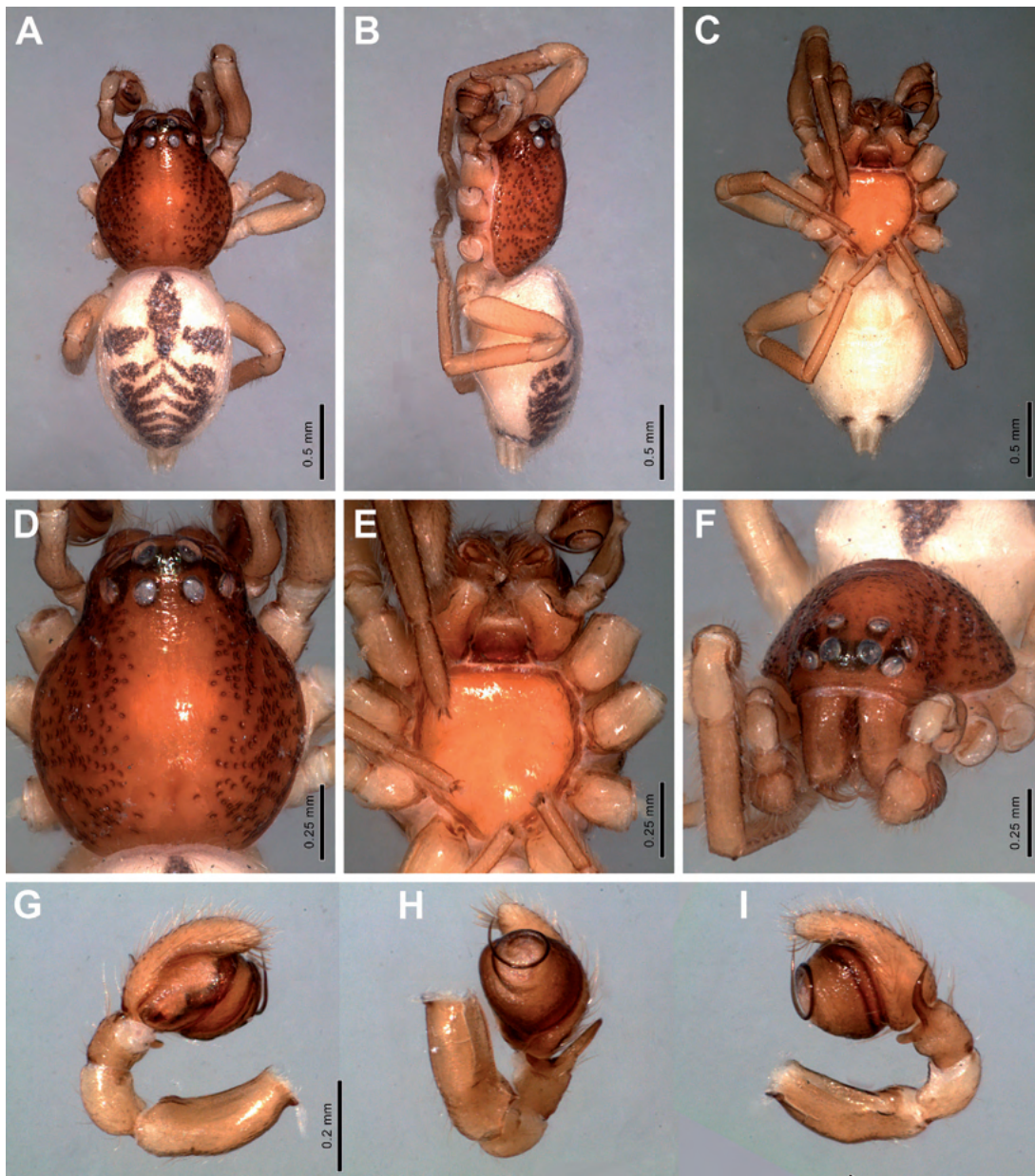


Fig. 14. *Paranita inesae*, new species, holotype male (MACN-Ar 43412). (A) habitus dorsal; (B) same, lateral; (C) same ventral; (D) carapace, dorsal view; (E) prosoma, ventral view; (F) prosoma, anterior view; (G) left male palp, prolateral view; (H) same, ventral view; (I) same, retrolateral view.

Diagnosis. Females of *P. inesae* can be easily distinguished from those of *P. paulae* by the short copulatory ducts and larger secondary spermatheca (Figs. 13D), as well as the copulatory openings in the center of the epigynal plate. The males can be distinguished by the nearly spherical copulatory bulb with shorter, coiling embolus (Fig. 13A–C, 14G–I), while in *P. paulae* the bulb

is flat and the embolus is much larger.

Description. Male. (Holotype). Measurements: CL 1.08, CW 0.9, AL 1.24, AW 0.90, TL 2.30, PERW 0.44, MOQAW 0.22, MOQPW 0.22, MOQL 0.20. Length of leg segments: I 0.74 + 0.32 + 0.60 + 0.44 + 0.28 = 2.38; II missing; III 0.56 + 0.26 + 0.40 + 0.44 + 0.22 = 1.88; IV 0.76 + 0.28 + 0.76 + 0.64 + 0.28 = 2.72. Ca-

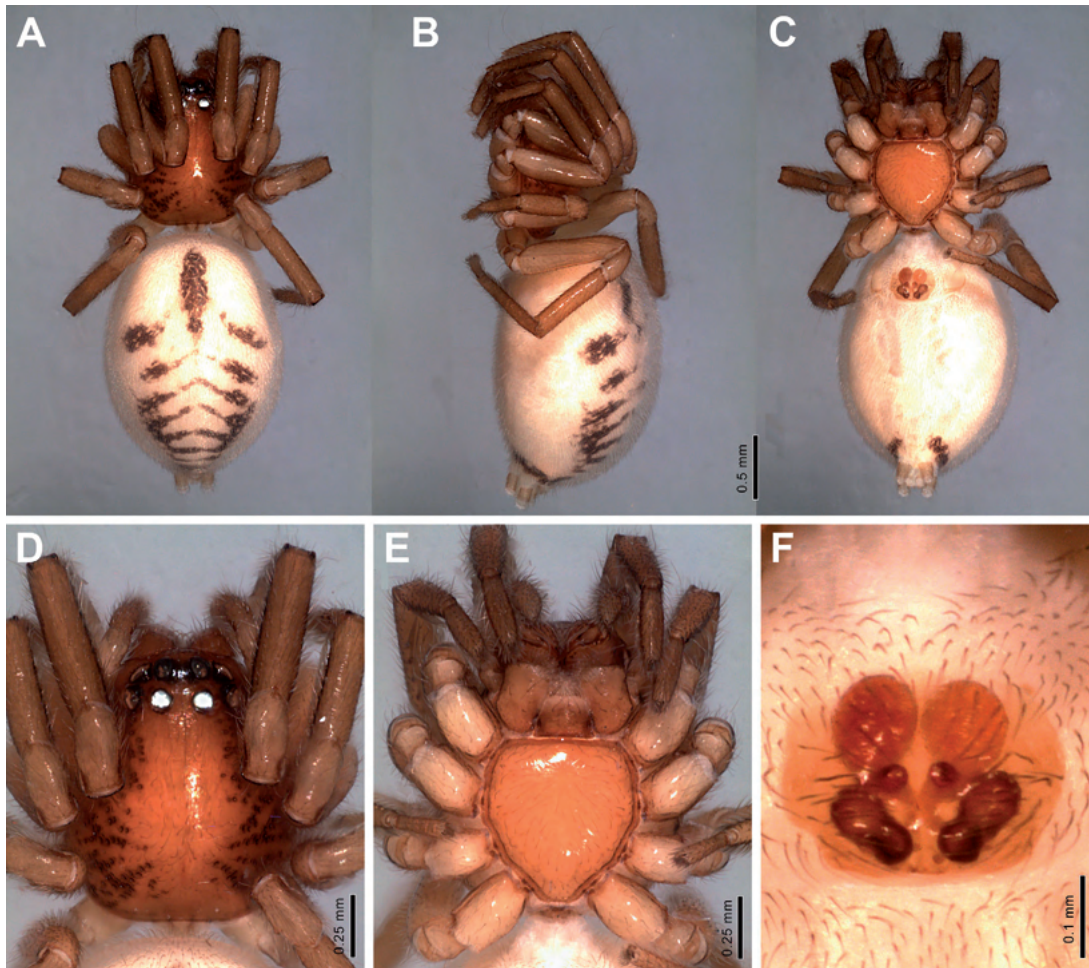


Fig. 15. *Paranita inesae*, new species, paratype female (MACN-Ar 13384). (A) habitus dorsal; (B) same, lateral; (C) same ventral; (D) carapace, dorsal view; (E) prosoma, ventral view; (F) epigyne, ventral view.

rapace pits covering mostly the lateral areas, leaving smooth cuticle along a wide median area (Fig. 14A). Colour: carapace deep orange-brown; chelicerae orange-brown; endites slightly paler than chelicerae, cream distally; labium brown; sternum smooth, uniform light orange, slightly darker at margins; palps and legs light brown; abdomen white dorsally with dark grey pattern: an anteromedian lanceolate cardiac patch and two transverse lateral bands followed by dorso-lateral chevron that expands caudally as an open ring around the spinnerets; venter and spinnerets whitish. Leg spination: femora and patellae spineless; both legs II missing (leg II spines from MACN-Ar 28353); tibiae: I plv 7 rlv 7, II pv 5/6 rlv 3/5 (asymmetrical); metatarsi: I plv 7 rlv 5, II plv 6, rlv 5; tarsi: I plv 3 rlv 3, II plv 4 rlv 2. Legs III and IV spineless, but with apical combs on

metatarsi. Palp (Figs. 13A–C, 14G–I): femur with longitudinal shallow furrow, patella unmodified; tibia relatively short, with a long, dorsally curved retrolateral apophysis, with pointed tip, and with additional ventral flattened short projection; bulb nearly spherical, embolus nearly filiform, with ventrodistal origin, describing one and half coils around distal part of tegulum, which appears less sclerotized distally.

Female. (Paratype, MACN-Ar 13384). Measurements: CL 1.12, CW 0.94, AL 1.92, AW 1.32, TL 3.00, PERW 0.46, MOQAW 0.22, MOQPW 0.24, MOQL 0.20. Length of leg segments: I 0.82 + 0.38 + 0.68 + 0.54 + 0.32 = 2.74; II 0.74 + 0.34 + 0.56 + 0.50 + 0.30 = 2.44; III 0.54 + 0.30 + 0.40 + 0.48 + 0.34 = 2.06; IV 0.84 + 0.32 + 0.66 + 0.76 + 0.34 = 2.92. Colour and sculpturing as in male, except by darker legs after coxae, and



Fig. 16. Geographic records of species of *Paranita*.

less profused abdominal pattern. Leg spination: femora and patellae spineless; tibiae: I plv 8/9 rlv 7, II plv 6 rlv 6; metatarsi: I plv 6 rlv 6, II plv 5 rlv 4; tarsi: I plv 3 rlv 3, II plv 3 rlv 3. Legs III and IV spineless, but with apical combs on metatarsi. Epigynal plate (Fig. 15F) pale orange, with internal structures visible through cuticle: copulatory openings circular, small, located centrally. Internal genitalia (Fig. 13D) consisting of three paired receptacles connected by relatively short copulatory duct; copulatory opening leads by short duct to large, spherical secondary spermatheca (S2), from there sclerotized distal copulatory duct (DCD) leads to oval receptacle of copulatory duct (RCD), and finally to spherical primary spermatheca (S1).

Type material. Holotype male from Argentina: Santa Fe Province: Vera Department: Las Gamas, 20 km W Vera [ca. S29.41382°, W60.37438°], Mar. 1995, P. Goloboff, M. Ramírez and C. Szumik, (MACN-Ar 43412). Paratypes: Argentina: Corrientes Province: San Cayetano Department: Estación Biológica de Corrientes (EBCo), S27.5526667°, W58.6789166° 49 m, 5–10 Nov. 2007, C. Grismado, L. Piacentini, M. Izquierdo, L. Compagnucci and J. Martínez, foliage beating, 1♀ (MACN-Ar 13384, vch CJG-2064), same data, 1♀ (MACN-Ar 13152, vch EMS-04042); San Cosme Department: Paso de la Patria [ca. S27.3173037°, W58.572589°], M. E. Galiano, Jan. 1966, 1♀ (MACN-Ar 43413); San Miguel, Colonia Montaña, Iberá, 28°3'S, 57°32'W, 6 Nov. 2017. G. Ávalos and C. Achitte, 1♂, 1♀ (together with 2

juvs., CARTROUNNE 9777).

Other material examined. Argentina. Corrientes Province: Mburucuyá: Parque Nacional Mburucuyá, Camino del Uno, S28.000999° W58.095255° (+/- 100 m), elev. 64 m, 27–30 May 2011, Rubio, G., Izquierdo, M. and Piacentini, L. Foliage beating, 1♂, 6♀, 2 juvs (MACN-Ar 28353). Chaco Province: Gral. Vedia, 26°56'1.5" S, 58°38'52.72" W, 10 Dec. 2014, G. Ávalos and C. Achitte, G-Vac, grassland, 1♀ (CARTROUNNE 9775).

Etymology. The specific name is in honor of Inés Ramírez Magariños, daughter of the first author, in homage for her love of small things with a cute design, like this spider species.

Distribution. Wetlands and grasslands in the Paraná River basin in Argentina, in Corrientes, Chaco and Sante Fe provinces (Fig. 16).

RELATIONSHIPS

The phylogenetic analysis of the concatenated dataset of sequence and morphology data under maximum likelihood (Fig. 17, S1) and parsimony (Fig. S2) coincided in the placement of *Paranita* in a clade together with the South American genera *Meriola* and *Trachelopachys* Simon, 1897, and the South African *Thysanina absolvo* Lyle and Haddad, 2006. Both analyses coincided in placing *Paranita* relatively far from the superficially similar species of *Orthobula* and *Capobula*, which also bear pits on the prosoma and series of long spines with tenent tips on the anterior

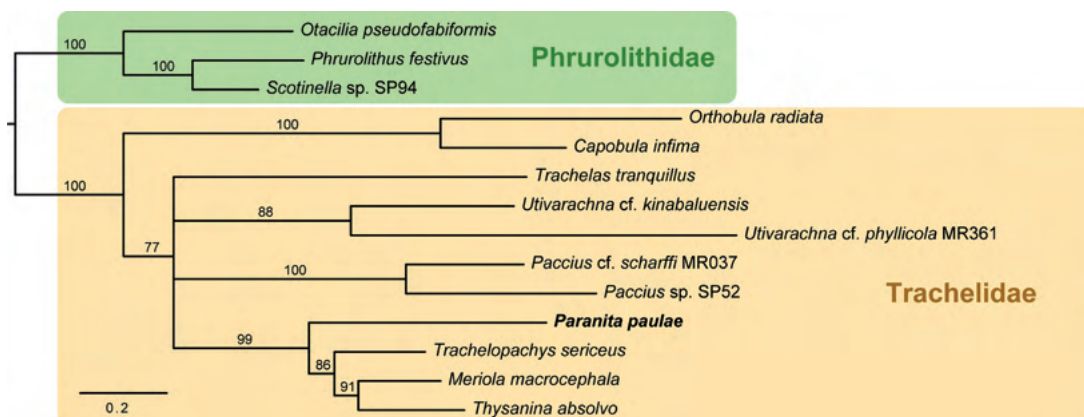


Fig. 17. Phylogenetic relationships of *Paranita* with representatives of Trachelidae and Phrurolithidae. Maximum likelihood analysis of concatenated dataset of six phylogenetic markers and morphology. Support values on branches are ultrafast bootstrap percentages; branches with support lower than 70 are collapsed. Scale bar = substitutions per site.

legs. All the genetic markers, in isolation or in combination, suggested this relationship (Figs. S3–S11). The morphological dataset analyzed in isolation (Figs. S11, S12) did not suggest a monophyletic group of *Paranita*, *Orthobula* and *Capobula*, despite the common characters mentioned above and other convergences, such as the absence of the thoracic fovea and the lateral projections of the claw lever pushing the bases of the claw tuft setae (Fig. 5G). The autapomorphies of *Paranita* are listed in Table 1, and the apomorphies of all groups and terminals are in Table S2.

DISCUSSION

Our phylogenetic analysis indicates that several remarkable similarities of *Paranita* with *Orthobula* and *Capobula* are indeed convergences: The pits on the prosoma, the anterior legs with series of long spines ending in a small tenent surface, and the detailed morphology of the claw lever. On close inspection, the pits of *Orthobula* and *Capobula* are round and have a central pore, seemingly revealing a secretory function (Ramírez, 2014; Haddad *et al.*, 2021, 2022), while those of *Paranita* are deep and elongate (Fig. 2G). Although we still have not seen if there are pores inside the pits in *Paranita*, they are probably secretory as well. In our phylogenetic tree, the leg spines are a plesiomorphy of *Orthobula*, because the closer outgroup, the Phrurolithidae, also have many ventral spines on the anterior legs. Whether *Paranita* have retained or convergently acquired the spines is ambiguous, because some tree resolutions of

the large polytomy in Figure 17 are compatible with an ambiguous optimization of the character. It is noteworthy that the tenent pad on the tip of the spines also occurs in some theumine Prodidomidae (species “cf. Moreno ARG”, see Ramírez, 2014; *Chileomma* Platnick, Shadab and Sorkin, 2005, see Rodrigues & Rheims, 2020), all small spiders that inhabit the leaf litter or grass bases. Other examples of setae with intermediate morphology between spines and scopular setae were reported in Liocranidae (see Ramírez, 2014: char. 155). These examples suggests that a transformation of scopular setae into spines might be a plausible evolutionary path that may have occurred in several clades.

CONCLUSION

We present a new genus of spiders from Argentina, associated with the grasslands and marshes in the floodplains of the Paraná and Uruguay river basins. This increases the trachelid spider fauna of Argentina and America to five genera, together with *Orthobula*, *Meriola*, *Trachelopachys* and *Trachelas*.

ACKNOWLEDGMENTS

We thank Martín Carboni (MACN) for the processing of bycatch markers from genomic data, and Silvia Adrián-Serrano (Institut de Recerca de la Biodiversitat, Universitat de Barcelona) for advice on this. Charles Haddad (Department of Zoology and Entomology, University of the Free State, South Africa) pro-

vided access to BOLD sequences of *Orthobula* and *Capobula*. The Administración de Parques Nacionales extended collection permits for work in Argentinian National Parks, as well as providing logistic support in the field. The Ministerio de la Producción de la Provincia de Santa Fe, Raúl Villasboas and Ivan Frigeri are acknowledged for hospitality in Estancia Las Gamas for fieldwork. Gustavo B. Scheidegger, director of Reserva Hotel “Amarran Sancho” for hospitality and logistic support, Sergio R. Zajarevich, director of Recursos Naturales, Ministerio de Producción, Trabajo y Turismo de la Provincia de Corrientes, for collection permits, and Martín Kowalewsky for logistic support and hospitality in Estación Biológica Corrientes. We thank all our co-collectors for help during field work. Gilberto Ávalos collected and loaned specimens from Corrientes. Charles Haddad, Jan Bosselaers and Luciano Patitucci provided useful corrections to an early version of this manuscript. This work was supported by grants PICT-2019-2745 from FONCyT and Fondo Fondo iBOL Argentina 2012 from CONICET.

Supplementary material

<http://revista.macn.gob.ar/ojs/index.php/RevMus/rt/suppFiles/824/0>

REFERENCES

- Allio, R., A. Schomaker-Bastos, J. Romiguier, F. Prosdocimi, B. Nabholz & F. Delsuc. 2020. MitoFinder: Efficient automated large-scale extraction of mitogenomic data in target enrichment phylogenomics. *Molecular Ecology Resources* 20(4): 892–905.
- Azevedo, G.F., T. Bougie, M. Carboni, M. Hedin & M.J. Ramírez. 2022a. Combining genomic, phenotypic and Sanger sequencing data to elucidate the phylogeny of the two-clawed spiders (Dionycha). *Molecular Phylogenetics and Evolution* 166(107327): 1–14.
- Azevedo, G.F., B. Tierney, M. Carboni, M. Hedin & M.J. Ramírez. 2022b. Convergence, hemiplasy, and correlated evolution impact morphological diversity related to a web-less lifestyle in the two-clawed spiders. *Insect Systematics and Diversity* 6(1): 1–14.
- Banks, N. 1895. A list of the spiders of Long Island; with descriptions of new species. *Journal of the New York Entomological Society* 3(2): 76–93.
- Bosselaers, J. & R. Jocqué. 2000. Studies in Corinnidae: transfer of four genera and description of the female of *Lessertina mutica* Lawrence 1942. *Tropical Zoology* 13(2): 305–325.
- Bosselaers, J. & R. Jocqué. 2002. Studies in Corinnidae: cladistic analysis of 38 corinnid and liocranid genera, and transfer of Phrurolithinae. *Zoologica Scripta* 31(3): 241–270.
- Briscoe, A.G., S. Goodacre, S.E. Masta, M.I. Taylor, M.A. Arnedo, D. Penney, J. Kenny & S. Creer. 2013. Can long-range PCR be used to amplify genetically divergent mitochondrial genomes for comparative phylogenetics? A case study within spiders (Arthropoda: Araneae). *PLoS one* 8(5): e62404.
- Cecarelli F.S., N. Mongiardino Koch, E.M. Soto, M.L. Barone, M.A. Arnedo & M.J. Ramírez. 2019. The grass was greener: Repeated evolution of specialized morphologies and habitat shifts in ghost spiders following grassland expansion in South America. *Systematic Biology* 68(1): 63–77.
- Deeleman-Reinhold, C.L. 2001. *Forest spiders of South East Asia: with a revision of the sac and ground spiders (Araneae: Clubionidae, Corinnidae, Liocranidae, Gnaphosidae, Prodidomidae and Tropchanteriidae [sic])*, Brill, Leiden, 591 pp.
- Goloboff, P.A. & S.A. Catalano. 2016. TNT version 1.5, including a full implementation of phylogenetic morphometrics. *Cladistics* 32(3): 221–238.
- González Márquez, M.E., C.J. Grismado & M.J. Ramírez. 2021. A taxonomic revision of the spider genus *Meriola* Banks (Araneae: Trachelidae). *Zootaxa* 4936(1): 1–113.
- Haddad, C.R. 2006. *Spinotrachelas*, a new genus of tracheline sac spiders from South Africa (Araneae: Corinnidae). *African Invertebrates* 47(1): 85–93.
- Haddad, C.R. & R. Lyle. 2008. Three new genera of tracheline sac spiders from southern Africa (Araneae: Corinnidae). *African Invertebrates* 49(2): 37–76.
- Haddad, C.R., C. Jin, N.I. Platnick & R. Booyens. 2021. *Capobula* gen. nov., a new Afrotropical dark sac spider genus related to *Orthobula* Simon, 1897 (Araneae: Trachelidae). *Zootaxa* 4942(1): 41–71.
- Haddad, C.R., C. Jin & N.I. Platnick. 2022. A revision of the spider genus *Orthobula* Simon, 1897 (Araneae: Trachelidae) in the Afrotropical Region. I. Continental species. *Zootaxa* 5133(3): 355–382.
- Hoang, D.T., O. Chernomor, A. von Haeseler, B.Q. Minh & L.S. Vinh. 2018. UFBoot2: Improving the ultra-fast bootstrap approximation. *Molecular Phylogenetics and Evolution* 35(2): 518–522.
- Kalyaanamoorthy, S., B.Q. Minh, T.K.F. Wong, A. von Haeseler & L.S. Jermiin. 2017. ModelFinder: Fast model selection for accurate phylogenetic estimates. *Nature Methods* 14(6): 587–589.
- Liang, Y., Q. Li, H.Q. Yin, H. Li & X. Xu. 2021. Two new species of the genus *Otacilia* from southern China (Araneae, Phrurolithidae). *Acta Arachnologica Siatica* 30(2): 99–105.
- Lyle, R. & C.R. Haddad. 2006. A revision of the Afrotropical tracheline sac spider genus *Thysanina* Simon, 1910 (Araneae: Corinnidae). *African Invertebrates* 47(1): 95–116.
- Lyle, R. & C.R. Haddad. 2010. A revision of the tracheline sac spider genus *Cetonana* Strand, 1929 in the Afrotropical region, with descriptions of two new genera (Araneae: Corinnidae). *African Invertebrates* 51(2): 321–384.
- Minh, B.Q., H.A. Schmidt, O. Chernomor, D. Schrempf, M.D. Woodhams, A. von Haeseler, & R. Lanfear. 2020. IQ-TREE 2: New models and efficient meth-

- ods for phylogenetic inference in the genomic era. *Molecular Biology and Evolution* 37(5): 1530–1534.
- Platnick, N.I. & C. Ewing. 1995. A revision of the tracheline spiders (Araneae, Corinnidae) of southern South America. *American Museum Novitates* 3128: 1–41.
- Platnick, N.I., M.U. Shadab & L.N. Sorkin. 2005. On the Chilean spiders of the family Prodidomidae (Araneae, Gnaphosoidea), with a revision of the genus *Moreno* Mello-Leitão. *American Museum Novitates* 3499: 1–31.
- Ramírez, M.J. 2014. The morphology and phylogeny of dionychan spiders (Araneae: Araneomorphae). *Bulletin of the American Museum of Natural History* 390: 1–394.
- Rodrigues, B.V.B. & C.A. Rheims. 2020. Phylogenetic analysis of the subfamily Prodidominae (Arachnida: Araneae: Gnaphosidae). *Zoological Journal of the Linnean Society* 190(2): 654–708.
- Shorthouse, D.P. 2010. SimpleMappr, an online tool to produce publication-quality point maps. Retrieved from <https://www.simplemappr.net>. Accessed August 21, 2023.
- Sica, Y.V., R.D. Quintana, V.C. Radeloff & G.I. Gavier-Pizarro. 2016. Wetland loss due to land use change in the Lower Paraná River Delta, Argentina. *Science of the Total Environment* 568: 967–978.
- Simon, E. 1897. Etudes arachnologiques. 27e Mémoire. XLII. Descriptions d'espèces nouvelles de l'ordre des Araneae. *Annales de la Société Entomologique de France* 65(1896): 465–510.
- Tockner K., S.E. Bunn, C. Gordon, R.J. Naiman, G.P. Quinn & J.A. Stanford. 2008. Flood plains: critically threatened ecosystems. In: N.V.C. Polunin (Ed.), *Aquatic ecosystems*, pp. 45–61. Cambridge University Press, Cambridge, UK.
- Wheeler, W.C., J.A. Coddington, L.M. Crowley, D. Dimitrov, P.A. Goloboff, C.E. Griswold, G. Hormiga, L. Prendini, M.J. Ramírez, P. Sierwald, L. Almeida-Silva, F. Alvarez-Padilla, M.A. Arnedo, L.R. Benavides, S.P. Benjamin, J.E. Bond, C.J. Grisaldo, E. Hasanal, M. Hedin, M.A. Izquierdo, F.M. Labarque, J. Ledford, L. Lopardo, W.P. Maddison, J.A. Miller, L.N. Piacentini, N.I. Platnick, D. Polotow, D. Silva-Dávila, N. Scharff, T. Szűts, D. Ubick, C.J. Vink, H.M. Wood & J. Zhang. 2017. The spider tree of life: Phylogeny of Araneae based on target-gene analyses from an extensive taxon sampling. *Cladistics* 33(6): 574–616.

Doi: 10.22179/REVMACN.26.824

Recibido: 7-VI-2023

Aceptado: 18-IX-2023